THE JOURNAL OF PHYSICAL CHEMISTRY B

Article

Double Proton Transfer Induced Twisted Intramolecular Charge Transfer Emission in 2-(4'-N,N-Dimethylaminophenyl)imidazo[4,5-b]pyridine

Anasuya Mishra, Saugata Sahu, Nihar Dash, Santosh Kumar Behera, and Govindarajan Krishnamoorthy

J. Phys. Chem. B, **Just Accepted Manuscript** • DOI: 10.1021/jp404472b • Publication Date (Web): 17 Jul 2013

Double Proton Transfer Induced Twisted Intramolecular Charge Transfer Emission in 2-(4'-*N*,*N*-Dimethylaminophenyl)imidazo[4,5-b]pyridine[#]

Anasuya Mishra, Saugata Sahu, Nihar Dash, Santosh Kumar Behera and G. Krishnamoorthy*

Department of Chemistry
Indian Institute of Technology Guwahati
Guwahati 781039, Assam
India

Ph: +91-3612582315

Fax +91-3612582349

Email: gkrishna@iitg.ernet.in

[#]Dedicated to Professor Robert S. H. Liu on his 75th birth anniversary

Abstract

The spectral characteristics of *N*,*N*-dimethyl-4-(4-methyl-4*H*-imidazo[4,5-b]pyridin-2-yl)benzenamine (PyN-Me), 1-methyl-2-(4'-(*N*,*N*-dimetylaminophenyl)imidazo[4,5-b] pyridine (ImNH-Me) and 2-phenylimidazo[4,5-b]pyridine (PIP) are investigated to understand the mechanism of protic solvent induced dual fluorescence of 2-(4'-*N*,*N*-dimethylaminophenyl)imidazo[4,5-b]pyridine (DMAPIP-b). No dual emission is observed from PyN-Me where pyridyl nitrogen is blocked from hydrogen bonding with protic solvents confirms the importance of hydrogen bonding of protic solvents with the pyridyl nitrogen in dual emission of DMAPIP-b. Like DMAPIP-b, ImNH-Me also exhibits weak emission and has shorter fluorescence lifetime in methanol. However single emission is observed from ImNH-Me in all solvents including protic solvents. This suggests that the imidazole hydrogen also plays a role in the dual emission process. The longer wavelength emission of DMAPIP-b in water increases with increase in pH of the solution owing to deprotonation of imidazole >NH group. Based on these results the mechanism for the dual emission of DMAPIP-b is proposed.

Keywords: dual fluorescence, ICT, hydrogen bond, proton coupled charge transfer

1. Introduction

Intramolecular charge transfer (ICT) has been a topic of growing interest both in photochemistry and photobiology as it is a possible mechanism for several biological processes and chemical energy conversion. In the donor acceptor system, upon excitation, transfer of charge takes place from the donor to the acceptor moiety which results in the formation of a highly dipolar state namely ICT state and emission takes place from both locally excited state and ICT state. Among various types of ICT process, the twisted ICT (TICT) process is a great area of interest.[1,2] In TICT model, the twisted geometry is favored where the donor moiety remains out of plane with respect to the acceptor moiety. Grabowski et al. suggested that the dual fluorescence observed in dimethylaminobenzonitrile in polar solvents are from the locally excited state and the TICT state.[1,2] The factors primarily responsible for the formation and stabilization of the TICT state are polarity, viscosity and hydrogen bonding.[2,3] The effects of polarity and viscosity of the medium on the TICT process are well established.[2] However the role of hydrogen bonding in the formation and stabilization of the TICT state is still not unambiguously established.[3] Studies of hydrogen bonding effects on the TICT process is a very active area of research.[3-9] Hydrogen bonding plays a very important role in the proton coupled charge transfer process which often observed in biological assemblies including photo system II and other photoprocesses.[10-14]

2-(4'-*N*,*N*-dimethylaminophenyl)imidazo[4,5-b]pyridine (DMAPIP-b, Chart 1) is a biologically active molecule and it acts as an inhibitor for Aurora-A, Aurora-B and Aurora-C kinases.[15] It also has interesting photophysical characteristics. Although, it emits single emission in nonpolar and polar aprotic solvents, it emits dual emission in polar protic medium.[16] Therefore, DMAPIP-b was used as a ratiometric probe to study

various microheterogeneous environments including protein.[17-19] However, despite the fact that the shorter wavelength emission and the longer wavelength emission are attributed to normal and TICT emission respectively, the mechanism for the formation of TICT state in protic environment is not clearly understood.

Fasani et al. first studied the amino derivative of DMAPIP-b, i.e. 2-(4'-aminophenyl)imidazo[4,5-b]pyridine and suggested that the hydrogen bonding of the protic solvent with imidazole nitrogen and its >NH group twist the imidazopyridine ring perpendicular to the rest of the molecule to form the TICT state.[20] This contradicts the commonly accepted model that the TICT state is formed by twisting of donor with respect to rest of the molecule and not by the twisting of the acceptor.[1,2] Yoon et al. also suggested that the hydrogen bonding of the solvent with acceptor makes it planar with spacer that facilitates the charge flow from the spacer to the acceptor.[4,5] In addition in Fasani et al. mechanism[20] the pyridyl nitrogen has no role in the formation of TICT state, which contradicts our results that the band maxima and the intensity of the longer wavelength emission are strongly perturbed by the position of the pyridyl nitrogen.[16] Therefore, to understand the mechanism of dual emission of DMAPIP-b, we have synthesized and investigated the photophysical characteristics of related molecules (Chart 1) *N*,*N*-dimethyl-4-(4-methyl-4*H*-imidazo[4,5-b]pyridin-2-yl)benzenamine (PyN-Me), *N*,*N*-dimethyl-4-(3-methyl-3H-imidazo[4,5-b]pyridin-2-yl)benzenamine or 1-methyl-2-(4'-(*N*,*N*-dimetylaminophenyl)imidazo[4,5-b]pyridine (ImNH-Me) and 2-phenylimidazo[4,5-b]pyridine (PIP).

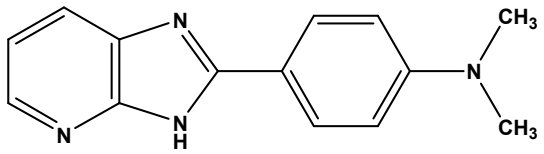

DMAPIP-b

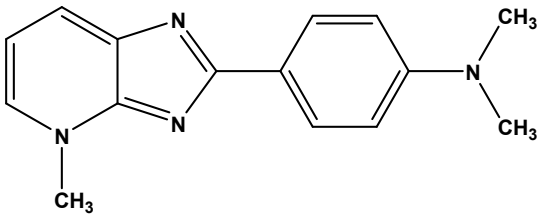

PyN-Me

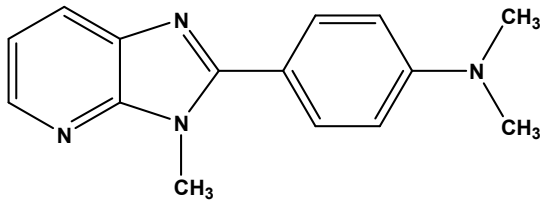

ImNH-Me

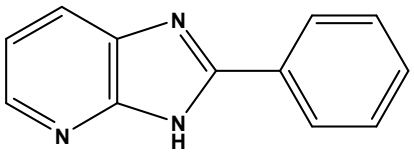

PIP

Chart 1. Structures of DMAPIP-b, PyN-Me, ImNH-Me and PIP.

2. Materials and methods

The synthetic procedure of DMAPIP-b is reported elsewhere,[16] and those of other molecules are given below:

Synthesis of *N*,*N*-dimethyl-4-(4-methyl-4*H*-imidazo[4,5-b]pyridin-2-yl)benzenamine (PyN-Me). PyN-Me was synthesized by irradiating the mixture of DMAPIP-b and methyl iodide by microwave (200 W) using the procedure given in the literature[21] and followed by a treatment with ammonia solution.[22] The compound was purified by preparative TLC. The identity of the compound was confirmed using NMR and mass spectra. ^{1}H NMR (400 MHz, $CDCl_3$, ppm) δ 7.71 (1H, d), δ 7.53 (2H, d), δ 7.26 (3H, m), δ 6.99 (1H, d), δ 4.19 (3H, s), δ 3.15 (6H, s). From LCMS the molecular mass (M + 1) was found to be m/z: 253.06.

Synthesis of 1-methyl-2-(4'-(*N*,*N*-dimetylaminophenyl)imidazo[4,5-b]pyridine (ImNH-Me). DMAPIP-b and methyl iodide (4:9 ratio) was dissolved in a solvent mixture of 3 ml dimethylformamide and 1 ml tetrahydrofuran. Powdered KOH was added and was heated at 40 °C for 24 hour by the procedure reported earlier for alkyl substitution of similar compounds.[23] The compound was extracted with dichloromethane and purified by column chromatography. The identity of the compound was confirmed by NMR and mass spectra. ^{1}H NMR (400 MHz, $CDCl_3$, ppm) δ 8.35 (1H, d), δ 8.02 (2H, d), δ 7.77 (1H, t), δ 7.22 (2H, d), δ 6.83 (2H, d), δ 4.00 (3H, s), δ 3.07 (6H, s). From LCMS the molecular mass (M + 1) was found to be m/z: 253.08.

Synthesis of 2-phenylimidazo[4,5-b]pyridine (PIP). PIP was synthesized by following the synthetic procedure of DMAPIP-b.[16] An equimolar mixture of 2,3-diaminopyridine (Aldrich) and benzoic acid (Aldrich) in polyphosphoric acid was heated at 230 °C for 3 h. The reaction mixture cooled to 100 °C and poured to excess ice cold water and neutralized with base. The compound was extracted with dichloromethane and purified by column chromatography. ^{1}H NMR (400 MHz, $CDCl_3$, and ppm) δ 8.41 (1H, d), δ 8.26 (2H, d), δ 8.15 (1H, d), 7.58 (3H, m), δ 7.30 (1H, m). From LCMS the molecular mass (M +1) was found to be m/z: 196.10.

Spectral measurements. Except glycerol (AR grade) all other solvents were HPLC grade from Rankem or Merck, India. The solvents were transparent in the spectral region of interest and were used as received. A Varian Cary 100 UV-visible spectrophotometer and a Horiba Jobin Yvon Spex Fluoromax 4 spectrofluorimeter were used to collect absorption and steady-state fluorescence spectra, respectively. For fluorescence measurements the absorbance of the solutions is kept ~ 0.1 at the absorption band maxima. The fluorescence quantum yields were measured with respect to quinine sulfate

in 1 N sulfuric acid (Φ_f = 0.55).[24] Time resolved fluorescence were measured using Edinburgh life spec II instrument, where the fluorescence lifetimes were determined by the method of time correlated single photon counting. A picosecond 375 nm laser diode was used as light source. The data were analyzed by reconvolution method by using the software provided by Edinburgh instrument.

Computational calculations. All the molecules are optimized in the ground state using gradient corrected exchange functional of Becke[25] and the correlation functional of Lee, Yang and Paar (LYP)[26] (B3LYP) using density functional theory (DFT) method and 6-31G(d,p) as the basis set. Vibrational frequency analyses were performed to confirm the minimum energy nature of the stationary points. Nowadays time dependent density functional theory (TDDFT) method becomes popular for electronic structure calculations in the excited states due to its moderate efficiency and accuracy.[27-30] The configuration interaction singles (CIS) predicts the geometries as well as molecular properties quite reasonably and correctly.[31-33] TDDFT calculations over CIS optimized geometries are efficient approach in predicting energy parameters for various systems.[34-38] We have performed TDDFT/B3LYP/6-31G(d,p) calculations on the optimized ground and excited states geometries to obtain the transition energies. All computational calculations were performed using Gaussian 03 software.[39]

3. Results and discussion

3.1. Absorption spectra of methyl derivatives

Table 1. Absorption band maxima (λ_{max}^{ab}, nm), fluorescence band maxima (λ_{max}^{fl}, nm) of PyN-Me, and ImNH-Me and DMAPIP-b[1]

Solvents	λ_{max}^{ab}			λ_{max}^{fl}		
	DMAPIP-b	PyN-Me	ImNH-Me	DMAPIP-b	PyN-Me	ImNH-Me
Cyclohexane	336, 352	333, 349, 366	323,332	359, 379, 398	373, 393, 419	362, 381, 401
Dioxane	340	346, 362	324,333	383	401	392
DMF	346	347, 361	337	428	402	414
DMSO		347, 362	339		403	421
Acetonitrile	345	343, 358	331	407	395, 430	412
Methanol	350	341, 355	335	414, 506	402	428
Ethanol	350	343, 356	336	413, 494	397	421
1-Propanol	349	343, 355	336	410, 486	398	418
2-Propanol	346	343, 356	336	408	395	415
Butanol	348	343, 357	336	407, 475	399	414
Glycerol	360	343, 356	343	446	406	441

[1]From ref. 16

To understand the role of pyridyl nitrogen and imidazole >NH group in the dual emission of DMAPIP-b, the methyl derivatives, PyN-Me and ImNH-Me (Chart 1) were synthesized. The absorption spectral data of methylated derivatives in different solvents are compared with DMAPIP-b in Table 1. The absorption spectra of all the three molecules are structured in nonpolar solvent. But in polar solvent the vibrational structure in the absorption spectra of ImNH-Me are blurred with a bathochromic shift as that of DMAPIP-b. However, in contrast to other two molecules, the absorption spectra of PyN-Me is more structured also in polar solvents. The absorption spectra of PyN-Me is less sensitive towards the polarity of the environment (7 nm shift). Whereas the solvatochromic shift in absorption spectra of ImNH-Me is comparatively larger (20 nm shift) than that of PyN-Me and comparable to that of DMAPIP-b (24 nm shift). Structureless absorption band in polar solvent and larger solvatochromic shift suggest

charge transfer in ImNH-Me. On the other hand, small solvatochromic shift and structured spectra indicate less charge transfer in PyN-Me.

Since, the multiparamateric approach of Kamlet et al. separates the different solvent parameters, it gives information about specific contribution of each solvent parameter.[40] Therefore, the absorption and the fluorescence spectral data are analyzed by multiple linear regression analysis to identify the different modes of solvation by employing the following equation.

$$E = E_0 + s\pi^* + a\alpha + b\beta$$

Where E is the absorption/fluorescence energy in cm^{-1}, E_0 is the value independent of solvent, π^* is the polarity/polarizability parameter of the solvents, α is the index of hydrogen bond donating ability of the solvent and β is the index of hydrogen bond accepting capacity of the solvent and *s*, *a* and *b* coefficients are the measure of sensitivities to each individual contributing parameter. The positive sign indicates the destabilization and negative sign indicates the stabilization of the system. The multiple linear regression analysis using the absorption spectral data result in following equations

$$E\ (\text{DMAPIP-b}) = 29860 - 966\ \pi^* - 900\ \alpha + 84\ \beta\ (r = 0.98)$$

$$E\ (\text{ImNH-Me}) = 31150 - 731\ \pi^* - 418\ \alpha - 802\ \beta\ (r = 0.96)$$

$$E\ (\text{PyN-Me}) = 28721 + 474\ \pi^* + 540\ \alpha - 271\ \beta\ (r = 0.96)$$

A good linear correlation is obtained for all the three molecules (regression ≥ 0.96). The value of E_0 obtained from this approach is also very good agreement with that of the experimental value in nonpolar cyclohexane. As expected due to charge transfer character the polarity/polarizability parameter stabilizes DMAPIP-b and ImNH-Me. In addition the hydrogen bond donating capacity of the solvent also stabilizes both DMAPIP-b and

ImNH-Me. On the other hand, in PyN-Me where the pyridine nitrogen is blocked and not available for hydrogen bonding, the coefficient of α becomes positive. Therefore, it is clear that the hydrogen bonding of the protic solvent with pyridine nitrogen stabilizes the molecule more than that with the imidazole nitrogen. Large negative values of '*s*' and '*a*' for DMAPIP-b indicate that the dipolar interaction and hydrogen bond donating ability of the solvent contribute more for the stabilization of DMAPIP-b than ImNH-Me.

3.2. Fluorescence spectra of methyl derivatives

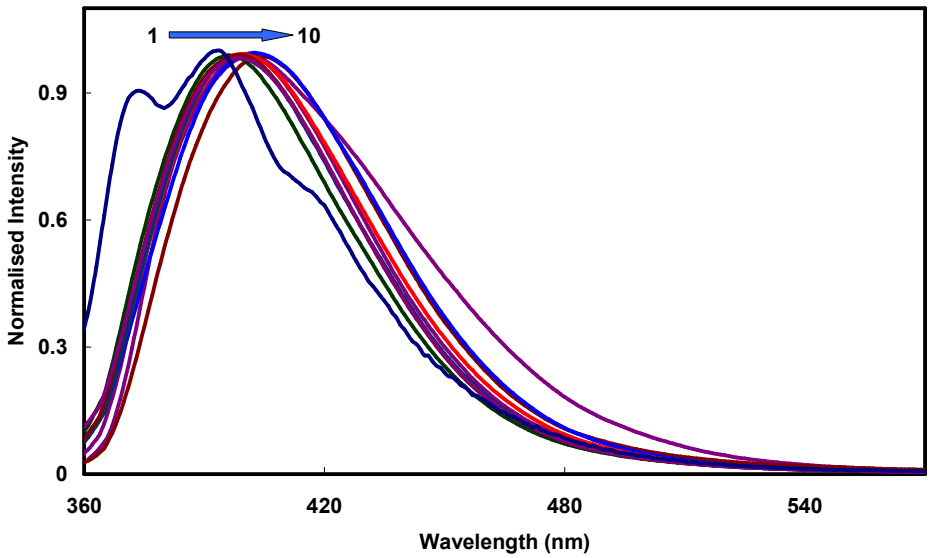

Figure 1. Normalised emission spectra of PyN-Me in different solvents: (1) cyclohexane, (2) 2-propanol, (3) 1-propanol, (4) butanol, (5) dioxane, (6) ethanol, (7) DMF, (8) methanol, (9) DMSO and (10) glycerol.

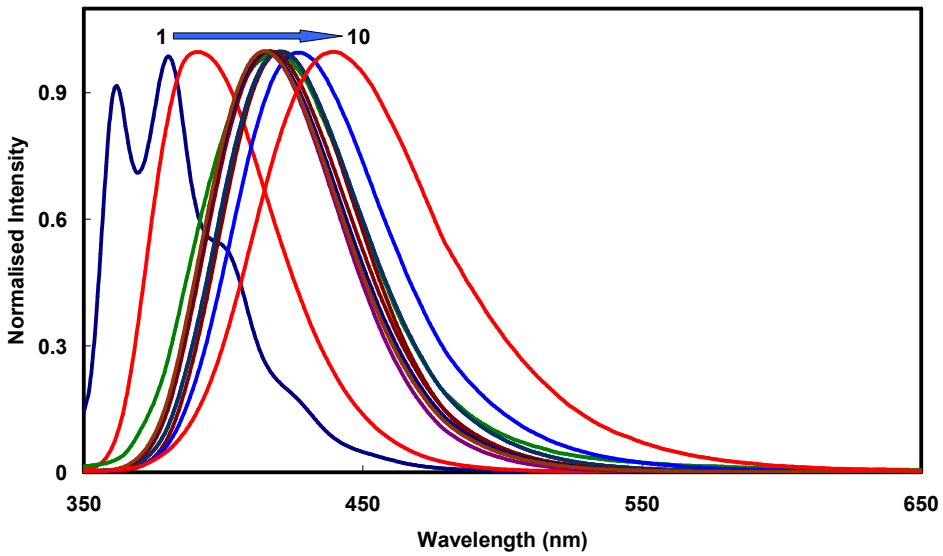

Figure 2. Normalised emission spectra of ImN-Me in different solvents: (1) cyclohexane, (2) dioxane, (3) 2-propanol, (4) DMF, (5) ethylene glycol, (6) n-propanol, (7) ethanol, (8) DMSO, (9) methanol and (10) glycerol.

Like DMAPIP-b, in methyl derivatives also the fluorescence spectra are structured in nonpolar solvents and upon increasing the polarity of the medium it becomes structureless with a red shift (Figure 1 and 2). The spectral shift of ImNH-Me is higher (60 nm) and is comparable to that of shorter wavelength emission of DMAPIP-b (67 nm). From this, it can be inferred that like in DMAPIP-b the locally excited state of ImNH-Me also has charge transfer character. On the other hand, the bathochromic shift is small in the fluorescence spectra of PyN-Me (13 nm) which indicates that PyN-Me is less sensitive towards the polarity of the medium.

The fluorescence spectral data are also analyzed by using SCM approach which result in the following equations.

$$E\ (\text{DMAPIP-b}) = 26900 - 2628\ \pi^* - 836\ \alpha - 593\ \beta\ (r = 0.93)$$

$$E\ (\text{ImNH-Me}) = 26453 - 2547\ \pi^* - 1922\ \alpha + 377\ \beta\ (r = 0.98)$$

E (PyN-Me) = 25210 - 318 π^* + 561 α - 476 β (r = 0.67)

The fluorescence spectral analysis also shows linear correlation in all the molecules and the values of E_0 also match well with the values in nonpolar solvent. As expected the contribution from π^* is also high for ImNH-Me and comparable to that of DMAPIP-b.

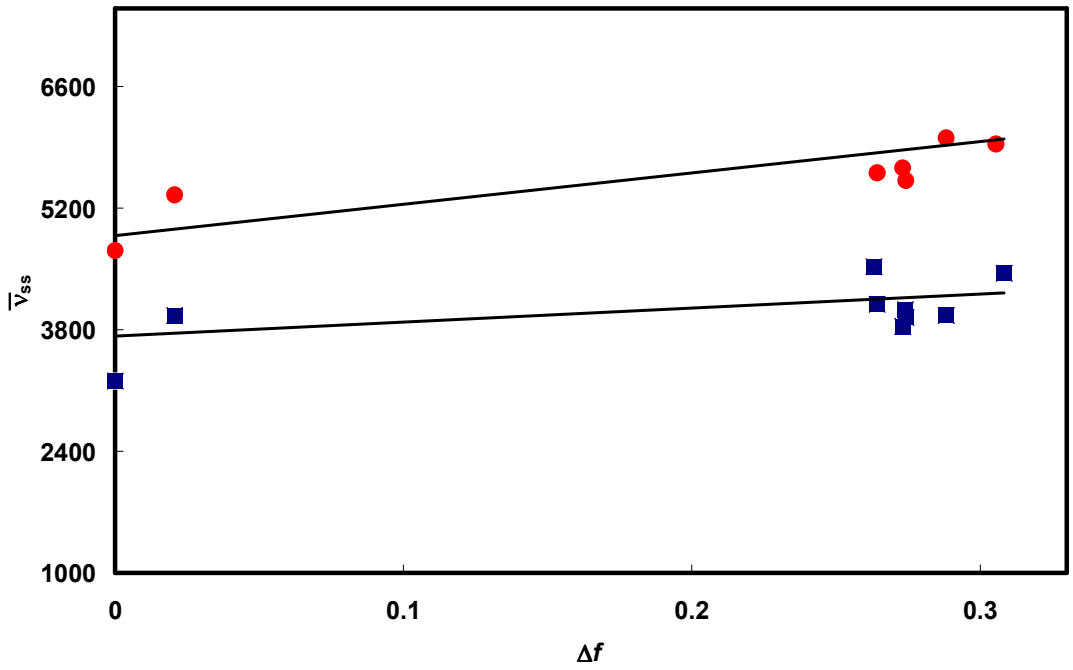

Figure 3. Lippert-Mataga plot for ImNH-Me (●) and PyN-Me (■).

Table 2. DFT optimized parameters of DMAPIP-b, ImNH-Me, PyN-Me and PIP

Molecules	Ground state Energy (eV)	Excitation energy[a] (eV)	Emission energy[a] (eV)	μ_g (D)	φ_1[b]	φ_2[b]
DMAPIP-b	-20707.0821	3.82 (3.69)	3.57 (3.27)	5.07	6.77 (3.23)	2.54 (0.11)
ImNH-Me	-21776.7682	3.88 (3.84)	3.53 (3.25)	4.77	7.70 (4.32)	29.3 (0.53)
PyN-Me	-21776.5134	3.16 (3.56)	3.09 (3.16)	2.64	0.04 (0.04)	0.00 (0.01)
PIP	-17061.3840	4.23 (4.04)	3.83 (3.65)	1.74		2.28 (0.02)

[a]values in parenthesis are experimental value in cyclohexane. [b]values in parenthesis are those of excited state. φ_1 - the torsional rotation of the dimethylamino group, φ_2 - torsional rotation of the dimethylanilino ring.

The Lippert-Mataga plot[41] was constructed for ImNH-Me, and PyN-Me (Figure 3) by using the relation

$$\bar{\nu}_{SS} = [2(\mu_e - \mu_g)/hca^3]\,\Delta f + \bar{\nu}_{SS}^{\circ}$$

here $\bar{\nu}_{SS}$ is the Stokes shift, the superscript "o" indicates the absence of solvent, μ_g and μ_e are dipole moments in the ground state and the excited state respectively, a is Onsager cavity radius. The Δf, the orientation polarizability is defined as

$$\Delta f = [(\varepsilon - 1) / (2\varepsilon + 1)] - [(n^2 - 1) / (2n^2 + 1)]$$

here ε and n are dielectric constant and refractive index of the solvent, respectively. The excited state dipole moments are estimated from the slope and the ground state dipole moment calculated by DFT method (Table 2). The excited state dipole moments thus obtained for ImNH-Me and PyN-Me are 11.24 D and 5.99 D, respectively. The excited state dipole moment of ImNH-Me is comparable to that of DMAPIP-b (12.20 D, small difference in excited state dipole moment with earlier value[16] due the small difference in the ground state dipole moment predicted by ab initio and DFT calculations).

Table 3. Fluorescence quantum yield (Φ_f) and life time (τ_f, ns) of methyl derivatives

Solvent	Φ_f		τ_f	
	PyN-Me	ImNH-Me	PyN-Me	ImNH-Me
Cyclohexane		0.82	1.22	1.17
Dioxane	0.39	0.89	1.27	1.42
Ethylacetate	0.34	0.29	1.28	1.31
DMF	0.45	0.93	1.41	1.61
DMSO	0.28	0.73	1.05	1.63
Acetonitrile	0.37	0.88	1.42	1.74
Methanol	0.47	0.22	1.78	0.57
Ethanol	0.45	0.81	1.67	1.87
1-Propanol	0.47	0.92	1.62	1.81
2-Propanol	0.43	0.93	1.58	1.87
Butanol	0.48	0.98	1.60	-

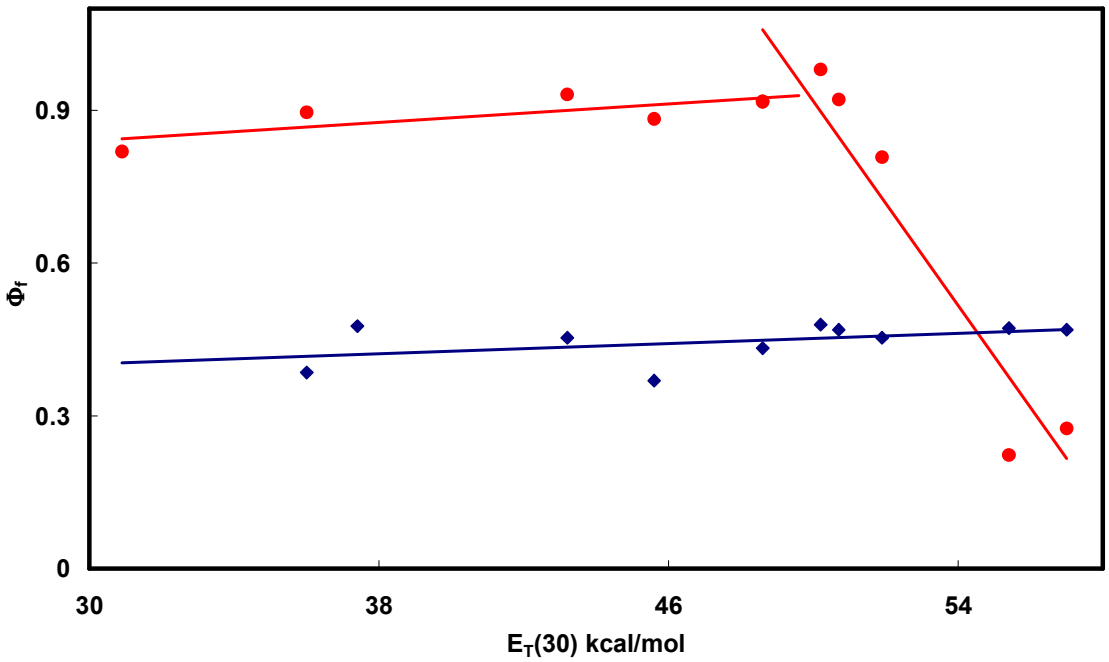

Figure 4. Plot of quantum yield versus $E_T(30)$ parameters for ImNH-Me (●) and PyN-Me (♦).

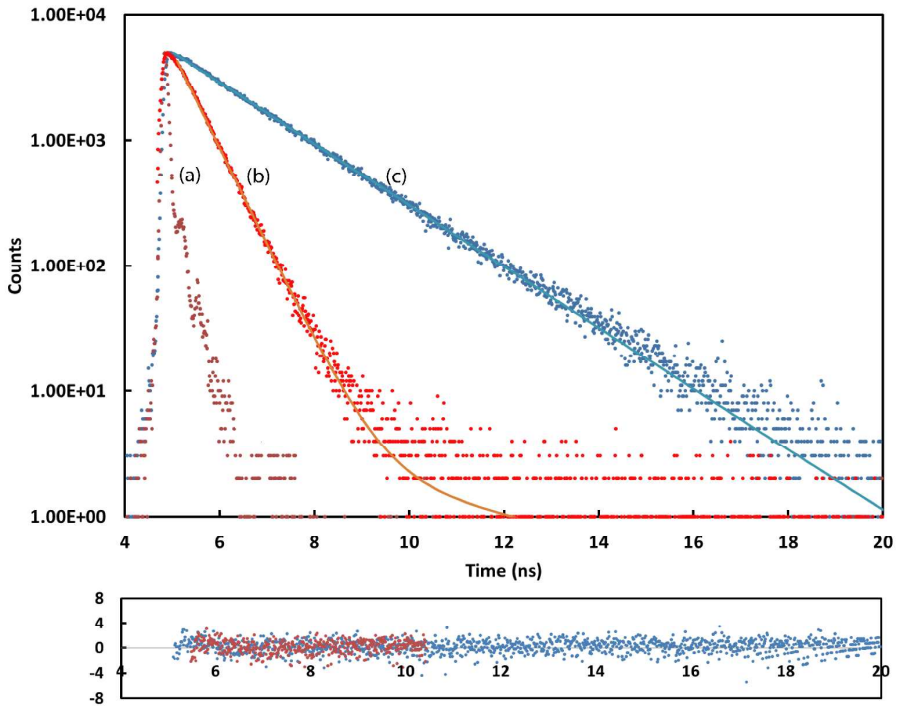

Figure 5. (a) The instrument response function and the fluorescence decays of (b) ImNH-Me and (c) PyN-Me in methanol along with fitted curves and residue plot.

The fluorescence quantum yields and the lifetime of methylated molecules are complied in Table 3 and the variation of quantum yield with $E_T(30)$ parameter is shown in Figure 4. The fluorescence quantum yield of PyN-Me varies very little with the nature of the environment. Whereas, the fluorescence quantum yields of ImNH-Me reduced in protic solvents and lowest in methanol. The fluorescence lifetime also attenuated in methanol (Figure 5 and Table 3). Same behavior is also observed for DMAPIP-b, whose shorter wavelength emission decay time is very low in methanol (0.31 ns) compared to other solvents (1.50 ns in acetonitrile).[16] But the fluorescence lifetime of PyN-Me in methanol is also comparable to those in other solvents. From this it can be inferred that the hydrogen bonding of the solvent with pyridyl nitrogen leads to fluorescence quenching.

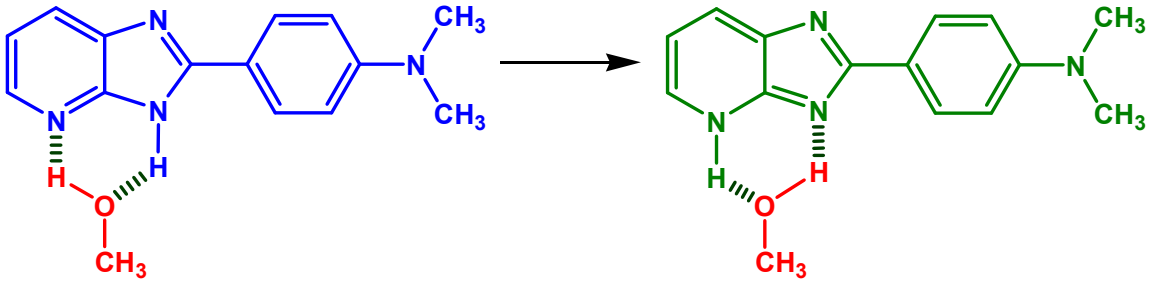

Scheme 1. Solvent assisted proton transfer.

Interestingly both methyl derivatives exhibit single emission not only in aprotic solvents but also in protic solvents. However, DMAPIP-b emits dual emission in protic solvents.[16] In PyN-Me, the pyridyl nitrogen is prevented from hydrogen bonding. On the other hand, in ImNH-Me, the imidazole >NH group is substituted by >N-Me and therefore >NH group is not available for hydrogen bonding. The absence of dual emission in PyN-Me and ImNH-Me show that both pyridyl nitrogen and >NH group are

vital for the dual emission of DMAPIP-b in protic solvents. One such possibility is transfer of proton from >NH group to pyridyl nitrogen to form tautomer (Scheme 1). Such solvent assisted inter molecular proton transfer in the excited state occurs in several molecules.[42-44]

3.3. Spectral characteristics of 2-phenylimidazo[4,5-b]pyridine

Table 4. Absorption band maxima (λ_{max}^{ab}, nm), fluorescence band maxima (λ_{max}^{fl}, nm) of PIP

Solvent	λ_{max}^{ab}	λ_{max}^{fl}
Cyclohexane	307, 321	324, 340, 358, 374
Dioxane	308, 321	328, 344, 360, 377
Ethylacetate	306, 320	326, 341, 357, 378
Ether	298, 307, 320	324, 340, 357, 374
DMF	308, 321	328, 343, 358, 377
Acetonitrile	307, 319	328, 343, 359, 378
Methanol	307, 320	328, 343, 358, 378
1-Propanol	306 (309) 320	328, 343, 359, 378
2-Propanol	307, 320	327, 341, 359,378
Butanol	307 (309) 321	328, 343, 358, 377
Glycerol	312, 322	332, 348, 362, 382

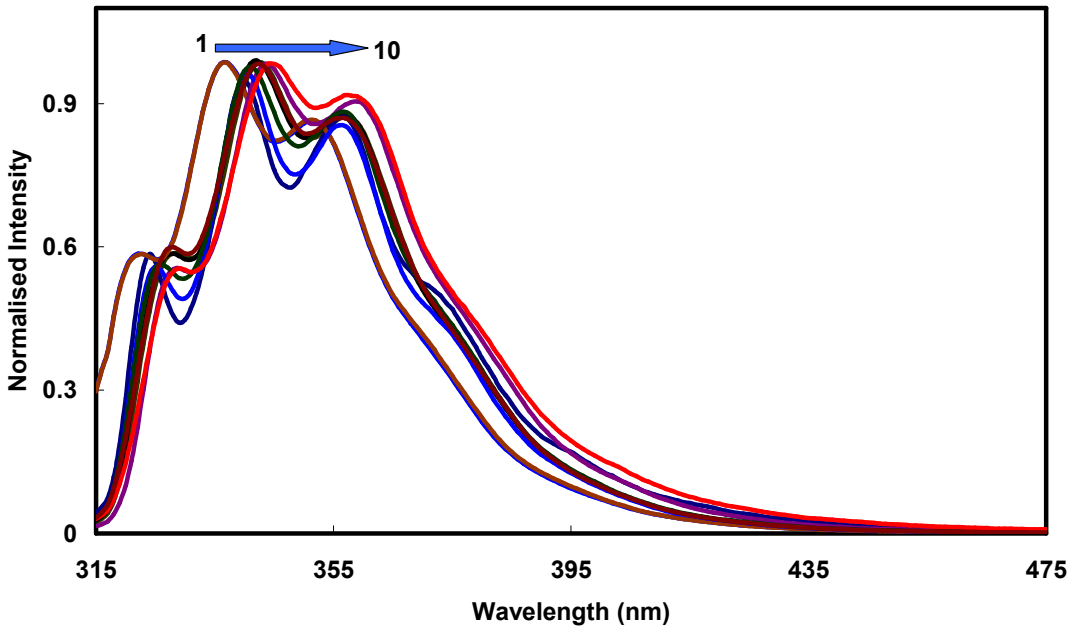

Figure 6. Normalised emission spectra of PIP in different solvents: (1) cyclohexane, (2) dioxane, (3) ether, (4) ethyl acetate, (5) DMF, (6) methanol, (7) 1-propanol, (8) 2-propanol, (9) butanol and (10) glycerol.

To verify the proton transfer hypothesis the spectral characteristics of PIP (Chart 1), the molecule without charge donor dimethylamino group, are investigated (Table 4). The absorption and the fluorescence band maxima are blue shifted compared to DMAPIP-b and the methylated derivatives due to the absence of charge donating dimethylamino group. The solvatochromic shift is also very small compared to other molecules and the fluorescence spectra also posses well resolved vibrational structure (Figure 6). Markedly no dual emission is observed in any solvent including protic solvents such as methanol. Despite the fact both pyridyl nitrogen and >NH group are freely available for hydrogen bonding, PIP exhibits single emission. Therefore, it can be concluded that the electron donating group is absolutely necessary for the dual emission in protic solvents and the longer wavelength emission originates from the charge transfer state. Further, strong positive solvatochromic of the longer wavelength emission of

DMAPIP-b and the higher dipole moment of it's emitting state (section 3.5) also substantiate the conclusion that the state is a charge transfer state.

3.4. Effect of deprotonation

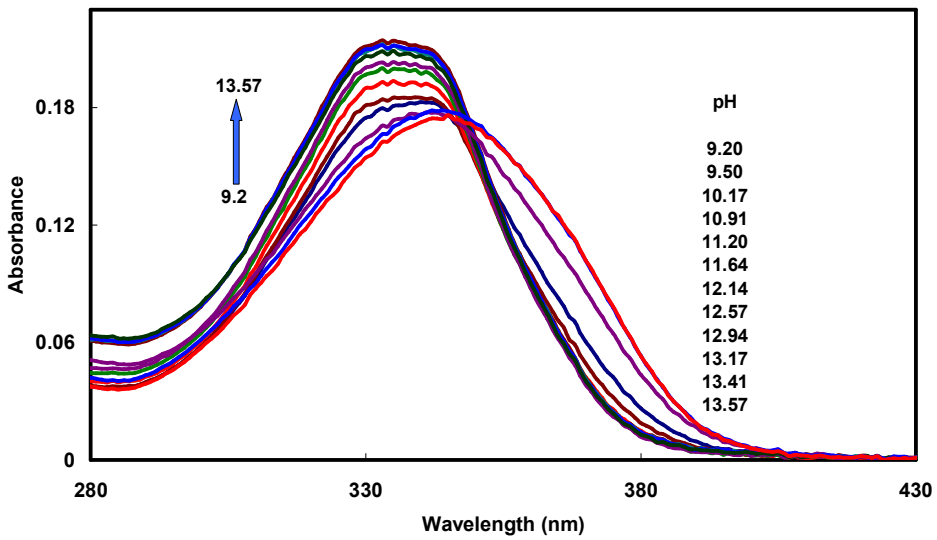

Figure 7. Absorption spectra of DMAPIP-b for neutral-anion equilibrium.

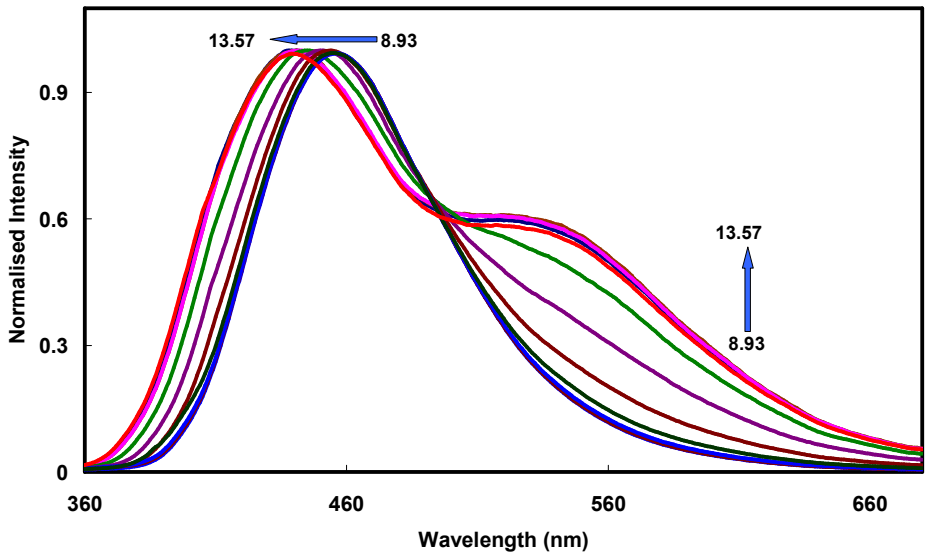

Figure 8. Normalised emission spectra (λ_{exc} = 349 nm) of DMAPIP-b for neutral-monoanion equilibrium.

To get further insight about the role of >NH proton in the dual emission, the neutral-anion equilibrium of DMAPIP-b was investigated. At pH 9.0 the molecule is in neutral form.[16] Upon increasing the pH the absorption spectrum is blue shifted with hyperchromic effect (Figure 7). DMAPIP-b has only one acidic proton (>NH). The spectral changes are consistent with the deprotonation of >NH group to form an anion. The blue shift is also observed in absorption spectra of similar molecules when the imidazole >NH group is deprotonated.[45,46] The effect of pH on the fluorescence spectra is shown in Figure 8. The fluorescence spectrum of DMAPIP-b has emission band in water at 451 nm with long tail. With increasing pH of the solution, the normal emission band is blue shifted. But the most interesting change is the emergence of longer wavelength emission upon deprotonation. At higher pH, two different lifetimes are observed for DMAPIP-b when monitored at 425 nm and 545 nm (Table 5). Compared to shorter wavelength when monitored at longer wavelength, the relative amplitude of the short lifetime species decreases while that of the long lifetime species increases. This indicates that the longer wavelength emitting state has longer lifetime and the shorter wavelength emitting species has shorter lifetime. This is consistent with the lifetimes of the neutral form of DMAPIP-b.[16] The observation of clear dual emission in anion suggests that the deprotonation may be one of the important step in the formation of longer wavelength emitting state in DMAPIP-b.

Table 5. Fluorescence lifetime (τ, ns) of the monoanionic form of DMAPIP-b and the values in parenthesis are relative amplitude

Monitoring wavelength (nm)	τ_1	τ_2	χ^2
425	0.37 (30.44)	2.79 (69.56)	1.05
545	0.39 (20.14)	2.81 (79.86)	0.95

3.5. Double Proton transfer induced TICT emission

The studies suggest that both pyridyl nitrogen and imidazole >NH group play important role in the dual emission of DMAPIP-b in protic solvents. The charge donor is absolutely essential and the longer wavelength emission is from charge transfer state. The dipole moment of the longer wavelength fluorescence emitting state was estimated by both solvatochromic (24.6 D) and thermochromic (25.5 D) methods.[47] The value is much higher than that of shorter wavelength emitting state (12.2 D). Based on the theoretical calculations, it was reported in the literature that the dipole moment of the TICT state is much higher than the planar ICT state.[48] Much higher dipole moment of the longer wavelength emitting state of DMAPIP-b clearly suggests that the ICT state is a TICT state. The enhanced dual emission in the anion reveals that the formation of TICT state in protic solvent involves the deprotonation of imidazole >NH proton. Based on these results we hypothesize that the formation of the TICT state is induced by solvent assisted (double) proton transfer from imidazole >NH to pyridyl nitrogen. The dissociation of proton from >NH group will produce a negative charge on the pyridyl nitrogen by resonance (Scheme 2), abstraction of proton by pyridyl nitrogen results in proton transfer. It is reported that the excited state intramolecular proton transfer is accompanied by a torsional rotation of the tautomer leads to formation of twisted charge transfer state in number of molecules.[38,49-52] However, in contrast to DMAPIP-b, the formation of tautomer in those systems is an intramolecular process and torsional motion of the tautomer often directs to nonemissive charge transfer state.

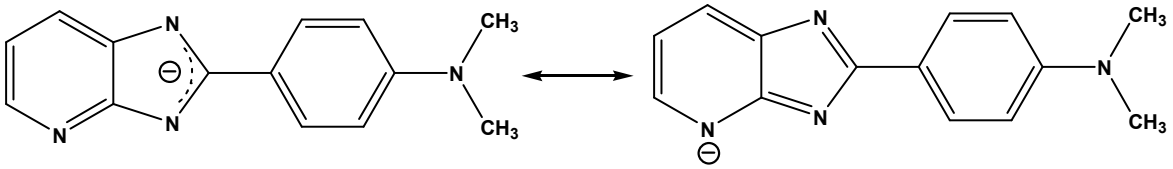

Scheme 2. Resonance stabilization of the anion form of DMAPIP-b.

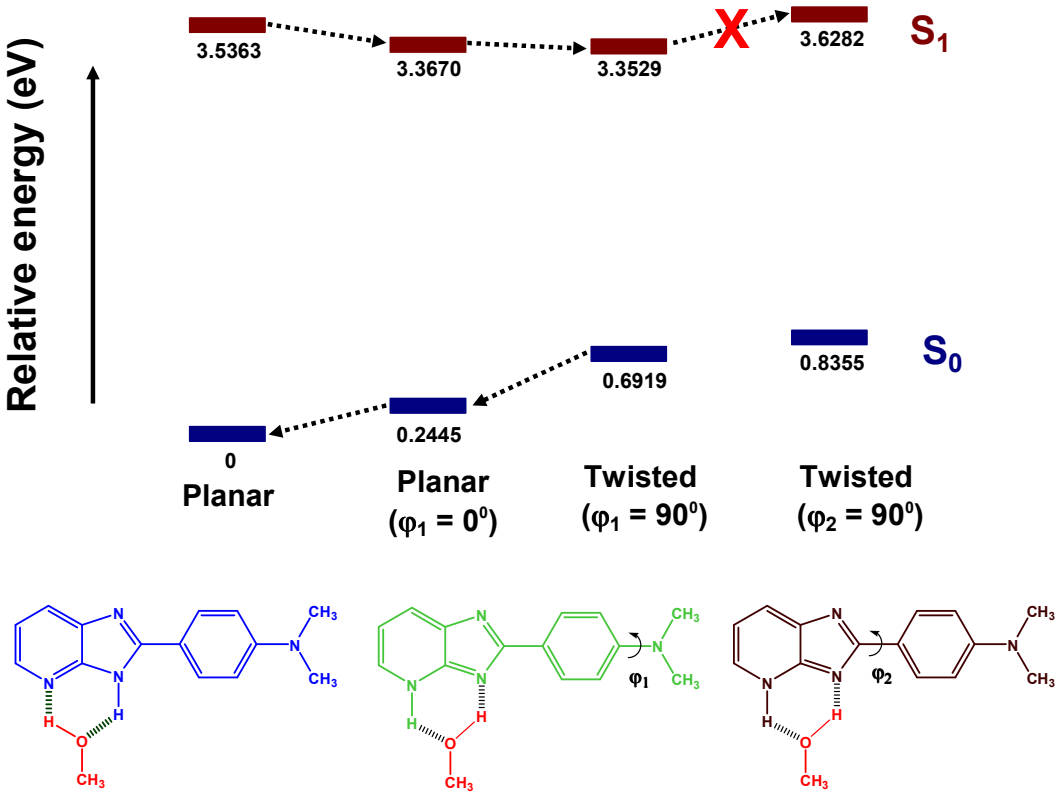

Scheme 3. Energy level diagram of different tautomer of DMAPIP-b.

To verify the hypothesis the structures of methanol-DMAPIP-b complexes are optimized and the energy level diagram was constructed (Scheme 3). The energy level diagram also shows that the excited state energy of the planar tautomer is less than that of normal form. The TICT state can be formed by rotation of either dimethylamino group or

dimethylaminophenyl ring. The calculations indicate that the energy of the dimethylaminophenyl ring twisted state is higher than that of the planar state and the energy of the twisted state is even higher than that of the locally excited state. Therefore, the formation of the TICT state by twisting of the dimethylaminophenyl ring is not a favored process. On the other hand, the energy of the dimethylamino group twisted state of the tautomer is lower than that of the planar state. This suggests that the TICT state is formed by the twisting of the dimethylamino group rather than the dimethylaminophenyl ring. The experimental emission energy of the longer wavelength fluorescence (2.46 eV)[16] is in better agreement with the emission energy predicted from the twisted state (2.66 eV) than the predicted energy from the planar state (3.12 eV).[16] This supports the proposed mechanism. Yoon et al. reported that the excited state proton transfer promotes the formation of TICT state in 4-*N*,*N*-dimethylaminosalylic acid and 4-aminosalylic acid.[53,54] They suggested that 4-aminosalylic acid which has weak electron donating group also emits TICT emission due to formation of phototautomer. They also demonstrated that the TICT emission of 4-*N*,*N*-dimethylaminosalylicacid is enhanced inside cyclodextrin cavity due to enhancement in the intramolecular hydrogen bond which favors the formation of phototautomer. Recently Guchhait et al. also proposed such proton transfer assisted charge transfer in some photochromic Schiff bases.[55] Nonetheless, in DMAPIP-b the formation of tautomer is a double proton transfer process assisted by protic solvent molecule not an intramolecular process.

4. Conclusion

Both PyN-Me and ImNH-Me exhibit single emission not only in aprotic solvents, but also in protic solvents. The absence of dual emission in PyN-Me where pyridyl nitrogen

is prevented from hydrogen bonding with protic solvents emphasizes that the hydrogen bonding with pyridine nitrogen is crucial for the dual emission of DMAPIP-b in protic solvents. On the other hand, the absence of dual emission in ImNH-Me suggests that the hydrogen bonding with hydrogen of imidazole >NH group is also playing an important role in the process. The absence of dual emission in PIP substantiates the conclusion that the longer wavelength emitting state is a TICT state. The enhancement of longer wavelength emission at higher pH illustrates that the formation of charge transfer state involves the deprotonation of imidazole >NH hydrogen. The dual emission of DMAPIP-b in protic solvents is due to the formation of TICT state that is induced by double proton transfer. The TICT state is formed by the twisting of the dimethylamino group. The energy level diagram obtained by theoretical calculation also supports the hypothesis.

Acknowledgement

The authors acknowledge department of science and technology (DST), India and council of scientific and industrial research (CSIR), India for the financial support. The authors also thank the Central Instruments Facility (CIF), Indian Institute of Technology Guwahati for the Life Spec II and NMR instruments.

Supporting Information:

Full authors list for references 28 and 39. This material is available free of charge via the Internet at http://pubs.acs.org.

References

1. Grabowski, Z. R.; Rotkiewicz, K.; Rettig, W. Structural Changes Accompanying Intramolecular Electron Transfer: Focus on Twisted Intramolecular Charge-Transfer States and Structures. *Chem. Rev*. **2003**, *103*, 3899–4031.
2. Rettig, W. Charge Separation in Excited States of Decoupled Systems—TICT Compounds and Implications Regarding the Development of New Laser Dyes and the Primary Process of Vision and Photosynthesis. *Angew. Chem., Int. Ed. Engl.* **1986**, *25*, 971-988.
3. Chipem, F. A. S.; Mishra, A.; Krishnamoorthy, G. Role of Hydrogen Bonding in Excited State Intramolecular Charge Transfer. *Phys. Chem. Chem. Phys.* **2012**, *14*, 8775–8790.
4. Cho, D. W.; Kim, H. Y.; Kang, S. G.; Yoon, M.; Kim, D. Cyclodextrin Effects on Excited-State Geometry Change and Intramolecular Charge Transfer of 4-Biphenyicarboxylic Acid. *J. Phys. Chem.* **1994,** *98*, 558–562.
5. Kim, Y.; Lee B. I.; Yoon, M. Excited-State Intramolecular Charge Transfer of *p*-*N*,*N*-dimethylaminobenzoic Acid in Y Zeolites: Hydrogen-Bonding Effects. *Chem. Phys. Lett*. **1998**, *286*, 466–472.
6. Zakharov, M.; Krauss, O.; Nosenko, Y.; Brutschy B. B.; Dreuw, A. Specific Microsolvation Triggers Dissociation-Mediated Anomalous Red-Shifted Fluorescence in the Gas Phase. *J. Am. Chem. Soc.* **2009**, *131*, 461–469.
7. Zhao, G.; Han, K. Time-dependent Density Functional Theory Study on Hydrogen-bonded Intramolecular Charge-transfer Excited State of 4-Dimethylamino-benzonitrile in Methanol. *J. Comput. Chem.* **2008**, *29*, 2010–2017.

8. Cazeau-Dubroca, C.; Lyazidi, S. A.; Cambou, P.; Peirigua, A.; Cazeau P.; Pesquer, M. Twisted Internal Charge Transfer Molecules: Already Twisted in the Ground State. *J. Phys. Chem.* **1989**, *93*, 2347–2358.
9. Owska, I. S.; Kubicki, J.; Herbich, J. Picosecond Kinetics of Excited-State Charge Separation in 4-(dimethylamino)pyridine. *Photochem. Photobiol. Sci.* **2005**, *4*, 106–112.
10. Cukier, R. L. Mechanism for Proton-Coupled Electron-Transfer Reactions. *J. Phys. Chem.* **1994**, *98*, 2377 - 2381 and related references listed therein.
11. Verkhovskaya, M.; Bloch, D. A. Energy-Converting Respiratory Complex I: On the Way to the Molecular Mechanism of the Proton Pump. *Int. J. Biochem. Cell Biol*. **2013**, *45*, 491–511.
12. Demchenko, A. P.; Tang, K.-C.; Chou, P.-T. Excited-State Proton Coupled Charge Transfer Modulated by Molecular Structure and Media Polarization. *Chem. Soc. Rev*. **2013**, *42*, 1379-1408.
13. Hammes-Schiffer, S. Theory of Proton-Coupled Electron Transfer in Energy Conversion Processes. *Acc. Chem. Res*. **2009**, *42*, 1881-1889.
14. Hsieh, C.-C.; Jiang, C.-M.; Chou, P.-T. Recent Experimental Advances on Excited-State Intramolecular Proton Coupled Electron Transfer Reaction. *Acc. Chem. Res.* **2010**, *43*, 1364-1374.
15. Bavetsias, V.; Sun, C.; Bouloc, N.; Reynisson, J.; Workman, P.; Linardopoulos, S.; Edward, M. Hit generation and exploration: imidazo[4,5-b]pyridine derivatives as inhibitors of Aurora kinases, Bioorg. *Med. Chem. Lett*. **2007**, *17*, 6567–6571.

16. Dash, N.; Chipem, F. A. S.; Swaminathan, R.; Krishnamoorthy, G. Hydrogen Bond Induced Twisted Intramolecular Charge Transfer in 2-(4'-Dimethylaminophenyl)imidazo[4,5-*b*]pyridine. *Chem. Phys. Lett.* **2008**, *460*, 119–124.

17. Dash, N.; Krishnamoorthy, G. Photophysics of 2-(4'-*N*,*N*-Dimethylaminophenyl)imidazo[4,5-b]pyridine in Micelles: Selective Dual Fluorescence in Sodium Dodecylsulphate and Triton X-100. *J. Fluoresc*. **2010**, *20*, 135–142.

18. Dash, N.; Chipem, F. A. S.; Krishnamoorthy, G. Encapsulation of 2-(4'-*N*,*N*-Dimethylamino)phenylimidazo[4,5-*b*]pyridine in β-Cyclodextrin: Effect on H-Bond-induced Intramolecular Charge Transfer Emission. *Photochem. Photobiol. Sci.* **2009,** *8*, 1708–1715.

19. Dash, N.; Mishra, A.; Krishnamoorthy, G. Alkyl Chain Dependent Interactions of Ligands with Bovine Serum Albumin. *J. Pharm. Biomed. Anal*. **2013**, *77*, 55-62.

20. Fasani, E.; Albini, A.; Savarino, P.; Viscardi G.; Barni, E. Hydrogen Bonding, Protonation and Twisting in the Singlet Excited State of Some 2-(4-aminophenyl)pyrido-oxa-, -thia-, And –imidazoles. *J. Heterocycl. Chem.* **1993**, *30*, 1041–1044.

21. Yu, H.; Kawanishi, H.; Koshima, H. Preparation and Photophysical Properties of Benzimidazole-Based Gels. *J. Photochem. Photobiol. A.* **2006**, *178*, 62–69.

22. Wu, F.; Chamchoumis, C. M.; Thummel, R. P. Bidentate Ligands that Contain Pyrrole in Place of Pyridine. *Inorg. Chem.* **2000**, *39*, 584-590.

23. Tong, Y. -P.; Zheng S. -L.; Chen, X. -M. Syntheses, Structures, Photoluminescence and Theoretical Studies of Two Dimeric Zn(II) Compounds with Aromatic N,O-Chelate Phenolic Ligands. *J. Mol. Struct.* **2007**, *826*, 104–112.

24. Crosby, A.; Demas, J. N. Measurement of Photoluminescence Quantum Yields. Review. *J. Phys. Chem.* **1971**, *75*, 991-1024.

25. Becke, A. D. Density-Functional Thermochemistry. 3. The Role of Exact Exchange. *J. Chem. Phys*. **1993**, *98*, 5648–5652.

26. Lee, C.; Yang, W.; Parr, R. G. Development of the Colle-Savetti Correlation-Energy Formula into a Functional of the Electron-Density. *Phys. Re*v. *B* **1988**, *37*, 785–789.

27. Zhao, G. J.; Han, K. L.; Stang, P. J. Theoretical Insights into Hydrogen Bonding and its Influence on the Structural and Spectral Properties of Aquo palladium(II) Complexes: Cis-(dppp)Pd(H2O)$_2^{2+}$, Cis-(dppp)-Pd(H2O)(OSO2CF3)$^+$ - (OSO2CF3)$^-$. *J. Chem. Theo. Comp.* **2009**, *5*, 1955-1958.

28. Aloise, S.; Pawlowska, Z.; Ruckebusch, C.; Sliwa, M.; Dubois, J.; Poizat, O.; Buntinx, G.; Perrier, A.; Maurel, F.; Jacques, P. et al. A Two-Step ICT Process for Solvatochromic Betaine Pyridinium Revealed by Ultrafast Spectroscopy, Multivariate Curve Resolution, and TDDFT Calculations. *Phys. Chem. Chem. Phys*. **2012**, *14*, 1945-1956.

29. Dhar, S.; Roy, S. S.; Rana, D.K.; Bhattacharya, S. Bhattacharya, S.; Bhattacharya, S. C. Tunable Solvatochromic Response of Newly Synthesized Antioxidative

Naphthalimide Derivatives: Intramolecular Charge Transfer Associated with Hydrogen Bonding Effect. *J. Phys. Chem. A* **2011**, *115*, 2216-2224.

30. Cao, J.; Wu, T.; Sun, W.; Hu, C. Time-Dependent Density Functional Theory Study on the Excited-State Hydrogen Bonding Strengthening of Photoexcited 4-amino-1,8-naphthalimide in Hydrogen-Donating Solvents. *J. Phys. Org. Chem.* **2013**, *26*, 289-294.
31. Foresman, J. B.; Head-Gordon, M.; Pople, J. A.; Frisch, M. J. Toward a Systematic Molecular Orbital Theory for Excited States. *J. Phys. Chem.* **1992**, *96*, 135-149.
32. Stanton, J. F.; Gauss, J.; Ishikawa N.; Head-Gordon, M. A Comparison of Single Reference Methods for Characterizing Stationary Points of Excited State Potential Energy Surfaces. *J. Chem. Phys.* **1995,** *103*, 4160.
33. Parusel, A. B. J.; Rettig, W.; Sudholt, W. A Comparative Theoretical Study on DMABN: Significance of Excited State Optimized Geometries and Direct Comparison of Methodologies. *J. Phys. Chem. A* **2002**, *106*, 804-815.
34. Shukla M. K.; Leszczynski, J. Time-Dependent Density Functional Theory (TD-DFT) Study of the Excited State Proton Transfer in Hypoxanthine. *Int. J. Quantum Chem.* **2005***,105*, 387-395.
35. Belletête, M.; Blouin, N.; Boudreault, P. –L. T.; Leclerc, M.; Durocher, G. Optical and Photophysical Properties of Indolocarbazole Derivatives. *J. Phys. Chem. A* **2006,** *110*, 13696-13704.
36. Chipem, F. A. S.; Chatterjee, S.; Krishnamoorthy, G. Theoretical Study on Photochemical Behavior of Trans-2-[4-(dimethylamino)styryl]benzothiazole. *J. Photochem. Photobiol. A*. **2010**, *214*, 121-127.

37. Chipem, F. A. S.; Dash, N.; Krishnamoorthy, G. Role of Nitrogen Substitution in Phenyl Ring on Excited State Intramolecular Proton Transfer and Rotamerism of 2-(2-hydroxyphenyl) benzimidazole: A Theoretical study. *J. Chem. Phys.* **2011**, *134*, 104308.

38. Gahungu, G.; Zhang, J. "CH"/N Substituted Mer-Gaq3 and Mer-Alq3 Derivatives: An Effective Approach for the Tuning of Emitting Color. *J. Phys. Chem. B* **2005,** *109*, 17762-17767.

39. Frisch, M. J.; Trucks, G. W.; Schlegel, H. B.; Scuseria, G. E.; Robb, M. A.; Cheeseman, J. R.; Montgomery, J. A.; Vreven, Jr. T.; Kudin, T. K. N.; Burant, J. C. et al. *Gaussian 03,Revision E.01*; Gaussian, Inc.: Wallingford, CT, **2004**.

40. Kamlet, M. J.; Abboud, J.-L.M.; Abraham, M.H.; Taft, R.W., Linear Solvation Energy Relationships. 23. A Comprehensive Collection of the Solvatochromic Parameters, π*, α, and β, and Some Methods for Simplifying the Generalized Solvatochromic Equation. *J. Org. Chem.* **1983**, *48*, 2877–2887.

41. Lippert, E. *Z. Elektrochem*. Spektroskopische Bestimmung Des Dipolmomentes Aromatischer Verbindungen Im Ersten Angeregten Singulettzustand. **1957**, *61*, 962-975.

42. Vetokhina, V.; Dobek, K. ; Kijak, M.; Kaminska, I. I.; Muller, K.; Thiel, W. R.; Waluk, J. ; Herbich, J. Three Modes of Proton Transfer in one Chromophore: Photoinduced Tautomerization in 2-(1H-Pyrazol-5-yl)pyridines, Their Dimers and Alcohol Complexes. *Chemphyschem*. **2012**, *13*, 3661-3671.

43. Yu, X. -F.; Yamazaki, S.; Taketsugu, T. Theoretical Study on Water-Mediated Excited-State Multiple Proton Transfer in 7-azaindole: Significance of Hydrogen Bond Rearrangement. *J. Phys. Chem. A* **2012**, *116*, 10566–10573.

44. Basaric, N.; Doslic, N.; Ivkovic, J.; Wang, Y.–H.; Veljkovic, J.; Mlinaric-Majerski, K.; Wan, P. Excited State Intramolecular Proton Transfer (ESIPT) from Phenol to Carbon in Selected Phenylnaphthols and Naphthylphenols. *J. Org. Chem.* **2013**, *78*, 1811-1823.

45. Krishnamoorthy, G.; Dogra, S. K. Spectral Characteristics of the Various Prototropic Species of 2-(4'- N,N-dimethylaminophenyl)pyrido[3,4-d]imidazole. *J. Org. Chem*. **1999**, *64*, 6566-6574.

46. Dey, J. K.; Dogra, S. K. Dual Fluorescence of 2-(4'-(N,N-dimethylamino)phenyl)benzothiazole and its Benzimidazole Analogue: Effect of Solvent and pH on Electronic Spectra. *J. Phys. Chem*.**1994**, *98*, 3638-3644.

47. Dash, N.; Krishnamoorthy, G. Effect of Temperature on the Spectral Characteristics of 2-(4-N,N-dimethylaminophenyl)imidazo[4,5-b]pyridine. *Spectrochim. Acta A* **2012**, *95*, 540-546.

48. Cogan, S.; Zilberg, S.; Haas, Y. The Electronic Origin of the Dual Fluorescence in Donor-Acceptor Substituted Benzene Derivatives. *J. Am. Chem. Soc*. **2006**, *128*, 3335-3345.

49. Va´zquez, S. R.; Rodrı´guez, C. R.; Mosquera, M.; Prieto, F. R. Excited-State Intramolecular Proton Transfer in 2-(3'-Hydroxy-2'-pyridyl)benzoxazole. Evidence of Coupled Proton and Charge Transfer in the Excited State of Some o-Hydroxyarylbenzazoles. *J. Phys. Chem. A* **2007**, *111*, 1814–1826.

50. Chipem, F. A. S.; Krishnamoorthy, G. Comparative Theoretical Study of Rotamerism and Excited State Intramolecular Proton Transfer of 2-(2'-Hydroxyphenyl)benzimidazole, 2-(2'-Hydroxyphenyl)imidazo[4,5-b]pyridine, 2-

(2'-Hydroxyphenyl)imidazo[4,5-c] pyridine and 8-(2'-Hydroxyphenyl)purine. *J. Phys. Chem. A* **2009,** *113,* 12063–12070.

51. Konoshima, H.; Nagao, S.; Kiyota, I.; Amimoto, K.; Yamamoto, N.; Sekine, M.; Nakata, M.; Furukawa, K.; Sekiya, H. Excited-State Intramolecular Proton Transfer and Charge Transfer in 2-(2'-hydroxyphenyl)benzimidazole Crystals Studied by Polymorphs-Selected Electronic Spectroscopy. *Phys. Chem. Chem. Phys*. **2012**, *14*, 16448-16457.
52. Douhal, A.; Fiebig, T.; Chachisvilis, M.; Zewail, A. H. Femtosecond Dynamics of a Hydrogen-Bonded Model Base Pair in the Condensed Phase: Double Proton Transfer in 7-azaindole. *J. Phys. Chem. A* **1998**, *102*, 1657-1660.
53. Kim, Y.; Yoon, M.; Kim, D. Excited-State Intramolecular Proton Transfer Coupled-Charge Transfer of p-N,N-dimethylaminosalicylic Acid in Aqueous β-Cyclodextrin Solutions. *J. Photochem. Photobiol. A*. **2001**, *138*, 167–175.
54. Kim,Y.; Yoon, M. Intramolecular Hydrogen Bonding Effect on the Excited-State Intramolecular Charge Transfer of p-Aminosalicylic Acid. *Bull. Korean Chem. Soc*. **1998**, *19*, 980–985.
55. Jana, S.; Dalapati, S.; Guchhait, N. Proton Transfer Assisted Charge Transfer Phenomena in Photochromic Schiff Bases and Effect of $–NEt_2$ Groups to the Anil Schiff Bases. *J. Phys. Chem. A* **2012**, *116*, 10948−10958.

Table of Content